

Analytical investigation of strain loading frequency effect on stress-strain-temperature relationship of shape-memory alloy

T. IKEDA

*Department of Aerospace Engineering
Nagoya University
Furo-cho, Chikusa-ku
Nagoya 464-8603, Japan
e-mail: ikeda@nuae.nagoya-u.ac.jp*

IN THIS PAPER A SET OF SIMPLE GOVERNING EQUATIONS of shape-memory alloys was derived by introducing some assumptions and a formula giving temperature variation was obtained by integrating one of the governing equations. The factors affecting the temperature variation depending on loading frequency were analytically investigated from the formula. The obtained temperature variation agreed qualitatively with the measured data. The calculated stress-strain-temperature relationship also agreed qualitatively with the measured data. It was found from the formula that the temperature vibrates sinusoidally and approaches a certain value asymptotically, and that the temperature variation is affected by the ratio of frequency to heat transfer and the ratio of latent heat to generated heat.

Key words: shape-memory alloy, phase transformation, frequency dependence, analytical investigation, thermo-mechanical properties.

Copyright © 2015 by IPPT PAN

1. Introduction

SHAPE-MEMORY ALLOYS (SMAs), having unique properties such as shape memory effect and superelasticity, are applied in a wide range of fields such as aerospace, medical and livingware [1, 2]. However, deformation behaviour based on phase transformation is complicated since it depends on temperature and loading frequency as well as loading history. Accordingly, to understand the mechanism of such complicated behaviour and to optimally design products including SMAs, fundamental experimental data and mathematical models are necessary and many experimental and mathematical studies are performed.

With respect to fundamental aspects, OTSUKA and WAYMAN [1] edited a book on shape-memory materials and OTSUKA and REN [3] presented a review of physical metallurgy including phase diagram, crystal structures, the mechanism of martensitic transformations, the effect of composition and thermomechanical treatment and so on. SHAW *et al.* [4–8] published a series of articles

on experimental characterization of TiNi SMA wires. They introduced thermo-mechanical phenomena occurring in SMA wires and tips in their experiments. As mentioned above, the properties of SMAs such as temperature, stress versus strain relationship and damping capacity are strongly affected by the loading frequency, which is observed in experiments [9–16]. Also, in Part 4 [7] thermomechanical coupling effects in superelastic SMA was presented and it was concluded that rate sensitivity during stress-induced transformation comes from heat transfer characteristics in the surrounding environment, latent heat exchanges and temperature-dependent transformation stress. Recently, YIN *et al.* [17] have performed systematic experiments for a superelastic SMA bar specimen over a wide range of strain loading frequencies in stagnant air and showed detailed transient and saturated stress and temperature response against the loading frequency.

Figures 1a and 1b, respectively, show stress versus strain curves and temperature difference from surrounding air versus strain curves of a TiNi-SMA wire with a diameter of 0.75 mm (Kantoc, material code EF3256) for the first cycle of cyclic strain loading. This cyclic test was performed with a fatigue test machine (Shimadzu EHF-FB10kN-10LA), and the temperature was measured by a T-type thermocouple with a diameter of 0.025 mm (OMEGA Engineering, COCO-001) fixed in the middle of the wire [15]. Before this measurement one hundred training cycles were given to suppress the transition of the wire properties due to initial plastic deformation. The black short dashed lines, the red chained lines, the blue dashed lines and the green line represent the relationships for loading frequencies of 0.001 Hz, 0.01 Hz, 0.1 Hz and 1 Hz, respectively. For the frequency of 0.001 Hz, since the temperature is assumed to vary little, the

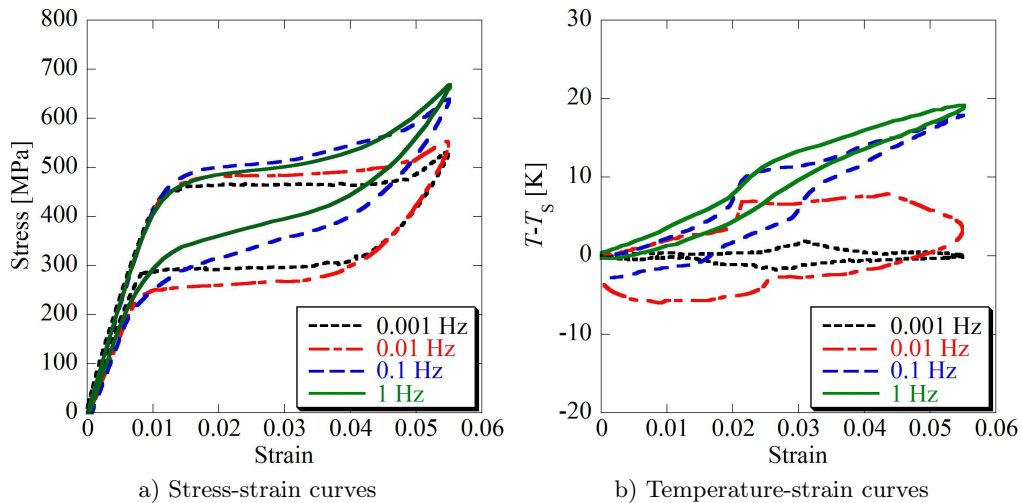


FIG. 1. Measured stress-strain-temperature curves for various loading frequencies.

stress keeps a constant value during the phase transformation in the stress versus strain curve. For the frequency of 0.01 Hz, since the temperature increases by 8 K from the surrounding air during the loading and decreases by 6 K during the unloading, the forward transformation stress becomes higher and the reverse transformation stress becomes lower than those for 0.001 Hz. For the frequencies of 0.1 Hz and 1 Hz, the temperature monotonically increases during the loading and monotonically decreases during the unloading, both the stress versus strain curves during the loading and the unloading become curves rising from the bottom left to top right. It is noted that the temperature increases after the cycle at 1 Hz, although it decreases after the cycle at other frequencies. Figures 2a and 2b show temperature variations for loading frequencies of 0.1 Hz and 1 Hz, respectively. The amplitude of the variation is about 10 K for both frequencies, and the mean temperature gradually decreases for 0.1 Hz while it increases for 1 Hz.

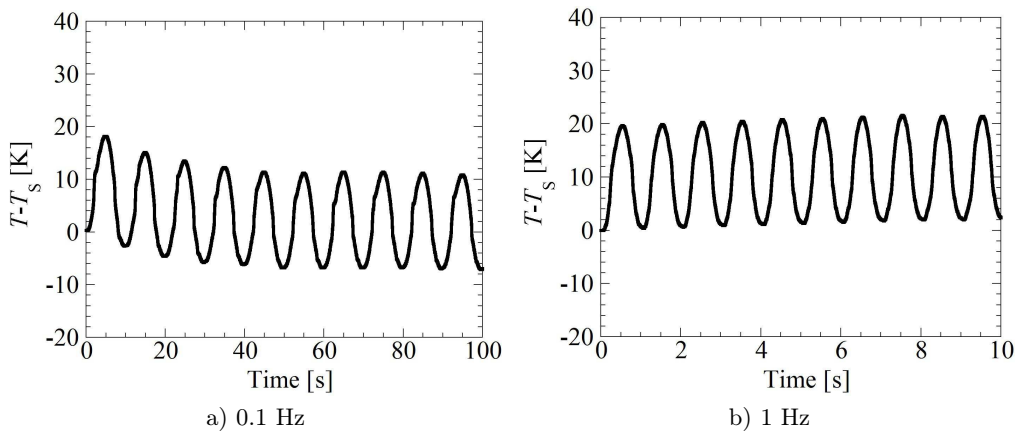


FIG. 2. Measured temperature variation.

As can be seen, the temperature variation changes depending on the loading frequency and it plays an important role in the deformation behaviour of SMAs. Accordingly, it is important to investigate the factors of the temperature variation analytically to predict the deformation behaviour.

To understand the phenomena observed in experiments and design systems including SMA elements, several types of constitutive models have been established [18, 19]. For example, FALK [20] proposed a model which obtains stress versus strain relationship by differentiating a free energy function assumed to be a polynomial of strain and temperature. MÜLLER [21] and SEELECKE [22] expressed the free energy function as the sum of free energy functions multiplied by a fraction of each phase and additionally introduced interfacial energy between the domains. These models cannot duplicate stable hysteretic behaviour because energy dissipation during phase transformation is not consid-

ered. BERTRAM [23], TANAKA [24], LIANG and ROGERS [25], BRINSON [26], SUN and HWANG [27], BOYD and LAGOUDAS [28], RANIECKI *et al.* [29], IVSHIN and PENCE [30], LECLERCQ and LEXCELLENT [31], KAMITA and MATSUZAKI [32], MATSUZAKI *et al.* [33], AURICCHIO and SACCO [34] and others have presented models which express the transformation process between martensitic phase and austenite phase or/and among martensitic variants by considering internal variables and the energy dissipation such as models in plastic deformation. The historical summary of these types of models was presented by MACHADO and LAGOUDAS [18]. PATOOR *et al.* [35], GALL and SEHITOGLU [36] and NAE *et al.* [37] presented models which obtain macroscopic behaviour by averaging variables in microscopic behaviour of individual grains where shape memory alloy was assumed to be composed of a number of grains. GRAESSER and COZZARELLI [38] and ORTÍN [39] drew hysteresis mathematically without respect to the detailed physical phenomena. As it is observed in the experiments the deformation behaviour strongly depended not only on temperature variation but also on loading-rate. Although many constitutive models are developed, most of them are temperature-dependent but rate-independent models. The effect of loading-rate can be discussed by taking into account an energy flow balance equation (a heat equation) in the temperature-dependent constitutive models [28 (adiabatic), 29, 30, 33, 34]. The energy flow balance equation, which will be shown later, is composed of the terms of temperature variation (sensible heat), heat sources (latent heat, thermoelastic effect and heat generation due to internal friction) and heat transfers (heat convection and heat conduction). Accordingly, the temperature variation is determined by the competition between the rate of heat release from the heat sources and the rate of heat transfer, and the rate-dependent stress versus strain relationship can be calculated by substituting the temperature variation into a temperature-dependent constitutive model.

IKEDA and his co-workers [37, 40–43] have proposed several types of constitutive models with an energy-based transformation criterion. To understand the behaviour of partial transformation theoretically, they proposed a grain-based micromechanical constitutive model [37]. By mathematically increasing the number of grains to infinity in the micromechanical model, another type of lumped parameter model referred to as the one-dimensional (1D) phase transformation model was obtained [40, in the paper this model was referred to as the shift and skip model]. Moreover, this model was extended so as to be able to describe tension-compression asymmetric behaviour [41, 42] and tension-torsion behaviour [43]. These models include the energy flow balance equation.

Figures 3a and 3b, respectively, show the comparison of stress versus strain curve [44] and temperature versus strain curves between the calculation obtained by using the 1D phase transformation model and the experimental data. The symbols represent the experimental data and the curves are the calculated values.

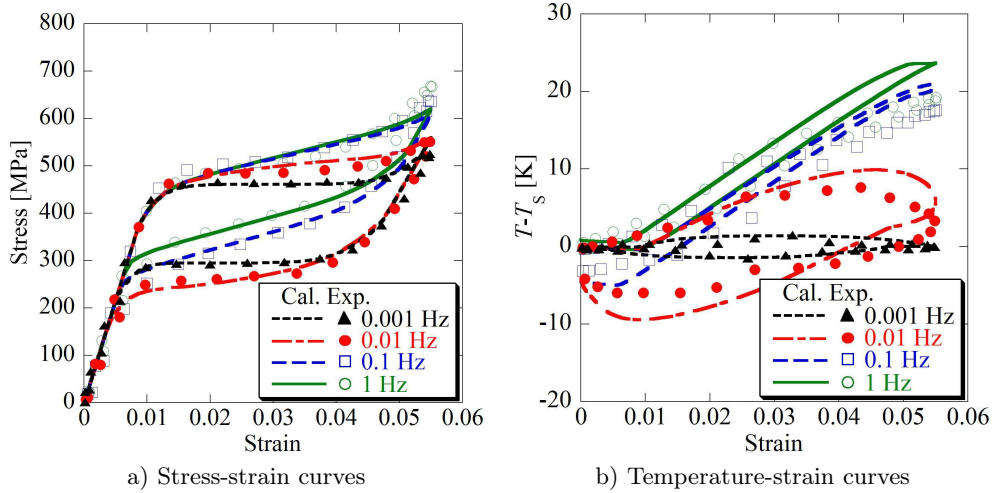


FIG. 3. Comparison of stress-strain-temperature curves between the 1D phase transformation model and the experiment.

It is seen that the 1D phase transformation model can quantitatively capture the features of the effect of loading frequency.

However, even though the 1D phase transformation model can quantitatively duplicate the stress-strain-temperature behaviour depending on the loading frequency, it is not clear what factors explicitly affect the temperature variation. HE and SUN [16] divided the cycle into five characteristic stages and solved the heat transfer equations for each phase of the stages. The five stages were: (1) elastic loading stage, (2) forward transformation stage, (3) elastic unloading stage, (4) reverse transformation stage and (5) elastic unloading stage. As a result the mean temperature variation and the amplitude depending on the strain rate were discussed. However, in the formulae it is still not easy to see the contribution of the parameters. YIN *et al.* [17] also analysed the temperature variation and the hysteresis loop area observed in their experiments. An explicit formulation of temperature was obtained from a simplified heat transfer equation by assuming sinusoidal strain loading and heat generation proportional to the square of the strain rate. To calculate the hysteresis loop area, Clausius–Clapeyron relationship with the calculated temperature was added to an isothermal stress versus strain relationship.

In this paper, in order to investigate the factors analytically, the 1D phase transformation model [40–43] is simplified by introducing some assumptions so that the temperature variation can be obtained by simple integration. Although explicit formulae of temperature and stress will be similar to YIN *et al.*'s formulae as a result, their derivations are different. Using the obtained formula,

general properties of the factors causing the temperature variation depending on the loading frequency are analysed by using normalized factors and frequency. Additionally, by using the temperature variation obtained by substituting typical material and environmental constants, the corresponding stress variation is calculated and validity of the simplified model is shown by comparing the calculated stress-strain-temperature relationship with the experimental data.

2. Governing equations

The governing equations, which can duplicate the thermodynamic behaviour of shape-memory alloys, are comprised of the following three equations [40–43]: the phase transformation criterion,

$$(2.1) \quad \frac{1}{2}\sigma^2\left(\frac{1}{E_\beta} - \frac{1}{E_\alpha}\right) + \sigma(\varepsilon_\beta - \varepsilon_\alpha) + (s_\beta - s_\alpha)(T - T_{\alpha\leftrightarrow\beta}) \\ = \Psi_{\alpha\rightarrow\beta}[z_{\alpha 1}] \\ = \Psi_{c1} + \Psi_{c2}\{1 - a_1^{-z_{\alpha 1}} + ba_2^{-(1-z_{\alpha 1})}\},$$

the constitutive equation,

$$(2.2) \quad \varepsilon = \sigma \sum_{\alpha} \frac{z_{\alpha}}{E_{\alpha}} + \sum_{\alpha} \varepsilon_{\alpha} z_{\alpha} + \alpha_T(T - T_s),$$

and the energy flow balance equation,

$$(2.3) \quad C \frac{dT}{dt} + \sum_{\alpha\rightarrow\beta} (s_\beta - s_\alpha) T \frac{dz_{\alpha\rightarrow\beta}}{dt} + \alpha_T T \frac{d\sigma}{dt} \\ = -h \frac{A}{V} (T - T_s) + \sum_{\alpha\rightarrow\beta} \Psi_{\alpha\rightarrow\beta} \frac{dz_{\alpha\rightarrow\beta}}{dt}.$$

In the above equations σ is the stress, E_{α} is the Young's modulus of phase α , ε_{α} is the intrinsic strain of phase α , s_{α} is the entropy of phase α , T is the temperature of the material, $T_{\alpha\leftrightarrow\beta}$ is the ideal reversible transformation temperature between phase α and phase β , $\Psi_{\alpha\rightarrow\beta}$ is the energy required when phase α transforms into phase β due to the dissipation such as internal friction and $z_{\alpha 1}$ is the variable related to the volume fraction of phase α . It is known that the required transformation energy can be approximated by the sum of two exponential functions in terms of the volume fraction. Ψ_{c1} , Ψ_{c2} , a_1 , b and a_2 are material constants and the set of the constants take each set of values for each transformation. In the constitutive equation ε is the strain, z_{α} is the volume fraction of phase α , α_T is the linear coefficient of expansion and T_s is the surrounding temperature. In the

energy flow balance equation C is the specific heat capacity, t is the time, $z_{\alpha \rightarrow \beta}$ is the volume fraction transforming from phase α to phase β , h is the coefficient of conduction and A/V is the area/volume. α and β are A for austenite phase or M for martensitic phase in this paper.

The transformation criterion means that during the transformation process the thermomechanical driving energy of the left-hand side is equal to the required transformation energy of the right-hand side. The strain is assumed to be the sum of the elastic strain, the transformation strain and the thermal strain. The energy flow balance equation is comprised of the sensible heat, the latent heat, the thermoelastic effect, the heat exchange between the SMA and the surrounding air and the heat generated due to the internal friction.

First, the phase transformation criterion is simplified. If it is assumed that $E_M = E_A = E$ and $\Psi_{A \rightarrow M} = \Psi_{M \rightarrow A} = \Psi = \text{constant}$, Eq. (2.1) is reduced to

$$(2.4) \quad \begin{cases} \sigma_{A \rightarrow M} \Delta \varepsilon - \Delta s (T - T_{\alpha \leftrightarrow \beta}) = \Psi, \\ -\sigma_{M \rightarrow A} \Delta \varepsilon + \Delta s (T - T_{\alpha \leftrightarrow \beta}) = \Psi, \end{cases}$$

and the transformation stresses are obtained as

$$(2.5) \quad \begin{cases} \sigma_{A \rightarrow M} = \frac{\Delta s}{\Delta \varepsilon} (T - T_{A \leftrightarrow M}) + \frac{\Psi}{\Delta \varepsilon}, \\ \sigma_{M \rightarrow A} = \frac{\Delta s}{\Delta \varepsilon} (T - T_{A \leftrightarrow M}) - \frac{\Psi}{\Delta \varepsilon}, \end{cases}$$

where $\Delta \varepsilon = \varepsilon_M - \varepsilon_A$ and $\Delta s = -(s_M - s_A)$.

Next, the constitutive equation is simplified. If it is assumed that $E_M = E_A = E$ and the thermal expansion is much smaller than the transformation strain, Eq. (2.2) is reduced to

$$(2.6) \quad \varepsilon = \frac{\sigma}{E} + \Delta \varepsilon z_M.$$

Finally, the energy balance equation is simplified. If it is assumed that $\Psi_{A \rightarrow M} = \Psi_{M \rightarrow A} = \Psi$, the thermoelastic effect is much smaller than the latent heat, the variation of martensite volume fraction is given by one minus cosine function as $z_M = 0.5\{1 - \cos(2\pi ft)\}$, the temperature variation is much smaller than the surrounding temperature and the heat generation rate is constant as $\Psi \pi f / 2$, Eq. (2.3) is reduced to

$$(2.7) \quad \frac{d\Theta}{dt} + H\Theta = S\pi f \sin(2\pi ft) + F \frac{\pi f}{2},$$

where f is the loading frequency,

$$\Theta = T - T_s, \quad H = \frac{hA/V}{C}, \quad S = \frac{\Delta s T_s}{C}, \quad F = \frac{\Psi}{C}.$$

If it is assumed that $\Theta = 0$ at $t = 0$ as the initial condition, Eq. (2.7) can be integrated as

$$(2.8) \quad \Theta = \Theta_1 e^{-Ht} + \Theta_2 \sin(2\pi ft - \phi) + \Theta_3,$$

where

$$\Theta_1 = \Theta_2 \sin \phi - \Theta_3, \quad \Theta_2 = \frac{S\pi f}{\sqrt{(2\pi f)^2 + H^2}} = \frac{S}{2} \frac{(2\pi f/H)}{\sqrt{(2\pi f/H)^2 + 1}},$$

$$\Theta_3 = \frac{F}{H} \frac{\pi f}{2} = \frac{F}{4} \left(\frac{2\pi f}{H} \right), \quad \phi = \tan^{-1} \left(\frac{2\pi f}{H} \right),$$

or they are rewritten as

$$\Theta_1 = \frac{S}{2} \sin^2 \phi - \frac{F}{4} \tan \phi, \quad \Theta_2 = \frac{S}{2} \sin \phi, \quad \Theta_3 = \frac{F}{4} \tan \phi$$

using ϕ .

3. Numerical example and discussion

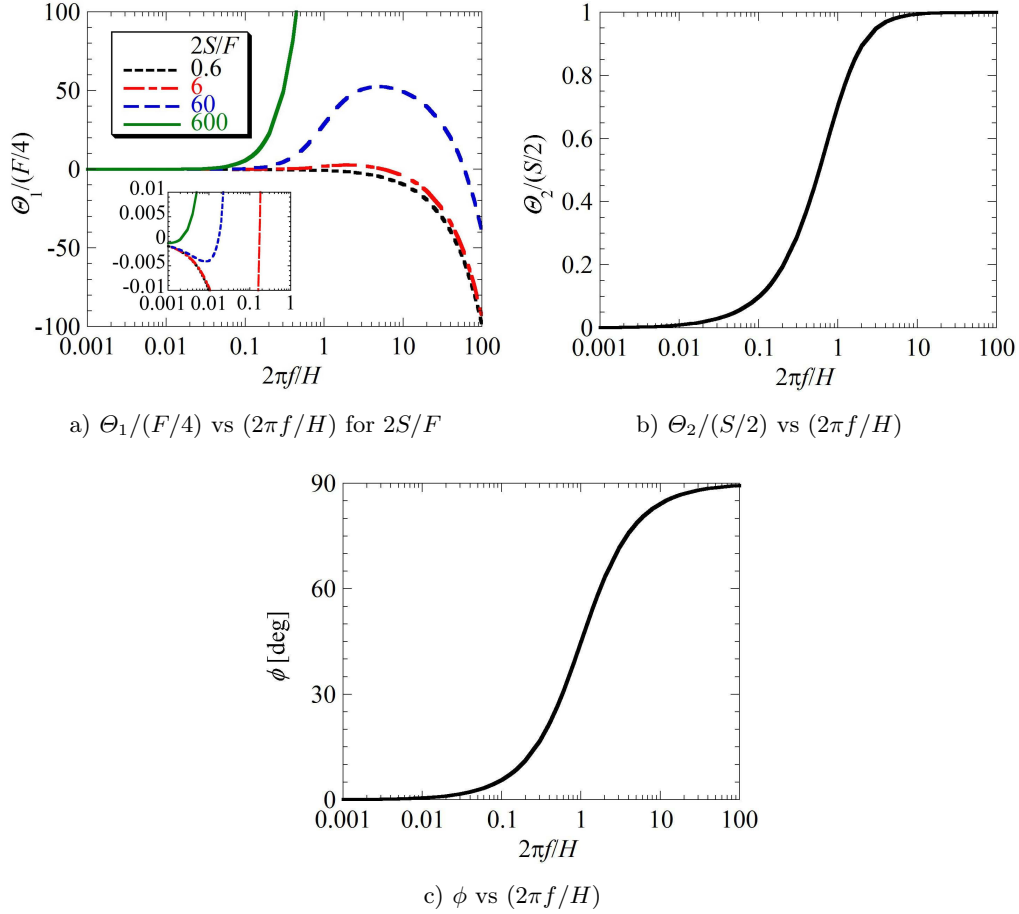
3.1. Analytical discussion

It is seen from Eq. (2.8) that the temperature vibrates sinusoidally and the mean temperature approaches a certain value asymptotically since the first term becomes 0 as $t \rightarrow \infty$ with a positive value of H .

Figures 4a, b and c show variation of $\Theta_1/(F/4)$, $\Theta_2/(S/2)$ and ϕ against $(2\pi f/H)$, respectively. Θ_1 is calculated from Θ_2 , Θ_3 and ϕ . The mean temperature decreases when Θ_1 is positive and increases when Θ_1 is negative. Θ_1 is zero and $d\Theta_1/d(2\pi f/H)$ is negative at $(2\pi f/H) = 0$ and $\Theta_1 \rightarrow -\infty$ as $(2\pi f/H) \rightarrow \infty$. When $2S/F$ is higher than 2, Θ_1 can take a positive value and the mean temperature decreases in the frequency range of

$$\frac{S}{F} - \sqrt{\left(\frac{S}{F}\right)^2 - 1} < \left(\frac{2\pi f}{H}\right) < \frac{S}{F} + \sqrt{\left(\frac{S}{F}\right)^2 - 1}.$$

Θ_2 is calculated from S , H and f . Θ_2 is the amplitude of the vibrating temperature, and it becomes larger as $(2\pi f/H)$ becomes higher and converges to $S/2$ as $(2\pi f/H) \rightarrow \infty$. It is noted that in this case since the temperature also goes to infinity (as will be explained later) the assumption that the temperature variation is much smaller than the surrounding temperature is no longer satisfied. Θ_3 is calculated from F , H and f , and proportional to $(2\pi f/H)$. Θ_3 is the mean temperature as $t \rightarrow \infty$. Here the mean temperature at $t=0$ is given by $\Theta_1 + \Theta_3$. ϕ is calculated from f and H , and it is the phase difference between the martensite volume fraction and the temperature. It is 0 degrees at $(2\pi f/H) = 0$ and becomes 90 degrees as $(2\pi f/H) \rightarrow \infty$.

FIG. 4. Variation of Θ_1 , Θ_2 and ϕ .

3.2. Numerical example

When material, shape and environmental conditions are assumed as listed in Table 1, H , S and F are calculated as listed in Table 2 and the values of Θ_1 , Θ_2 , Θ_3 and ϕ are calculated as listed in Table 3 for some loading frequencies. The values of the constants are roughly estimated based on the material and the environment in the experiment shown in Figs. 1 and 2 to examine qualitative behaviour by using the simplified governing equations.

It is seen from Table 3 that the amplitude of temperature is 14.8 K and the mean temperature decreases from 14.7 K at $t = 0$ and approaches asymptotically to 1.57 K as $t \rightarrow \infty$ for 0.1 Hz, and that the amplitude of temperature is 15.0 K and the mean temperature increases from 15.0 K at $t = 0$ to 15.7 K as $t \rightarrow \infty$ for 1 Hz. Figures 5a and 5b show the temperature variation at the frequencies

Table 1. Material, shape and environmental constants.

h [W/(m ² K)]	A/V [m ⁻¹]	C [MJ/(m ³ K)]	Δs [MJ/(m ³ K)]	T_s [K]
57	5.3×10^3	3	0.3	300
Ψ [MJ/m ³]	$T_{A \leftrightarrow M} - T_s$ [K]	$\Delta \varepsilon$	E [GPa]	
3	-40	0.03	30	

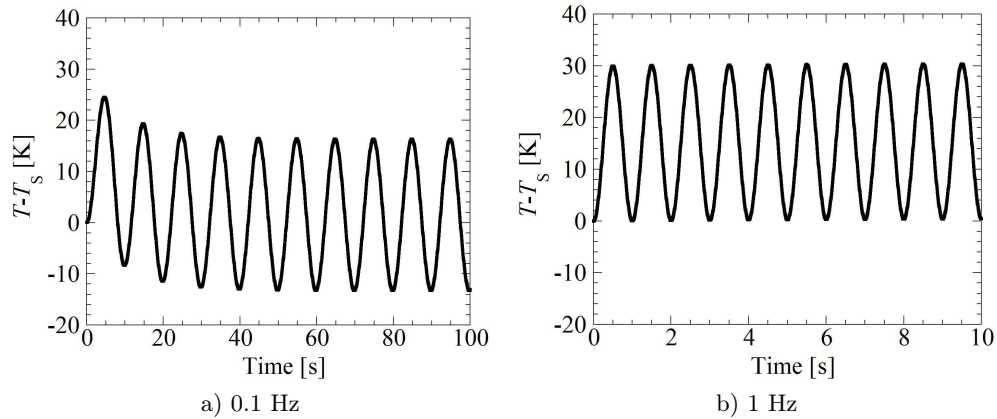
Table 2. Constants H , S and F .

H [s ⁻¹]	S [K]	F [K]
0.1	30	1

Table 3. θ_1 , θ_2 , ϕ and θ_3 for several loading frequencies.

f [Hz]	θ_1 [K]	θ_2 [K]	θ_3 [K]	ϕ [deg]
0.001	0.0433	0.941	0.0157	3.60
0.01	4.09	7.98	0.157	32.1
0.1	13.1	14.8	1.57	81.0
1	-0.712	15.0	15.7	89.1

of 0.1 Hz and 1 Hz, respectively, which are obtained from Eq. (2.8). This figure confirms the above mentioned trend. Comparing this analytical result with the experimental data shown in Figs. 2a and 2b, it is seen that this analytical solution using the simplified equation qualitatively captures the trend of the experimental data.

**FIG. 5. Calculated temperature variation.**

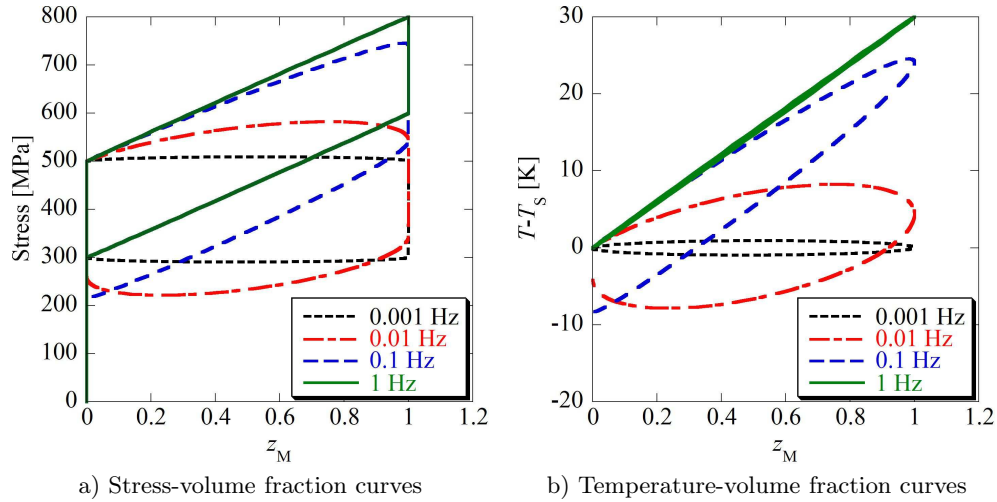


FIG. 6. Calculated stress-volume fraction-temperature curves for various loading frequencies.

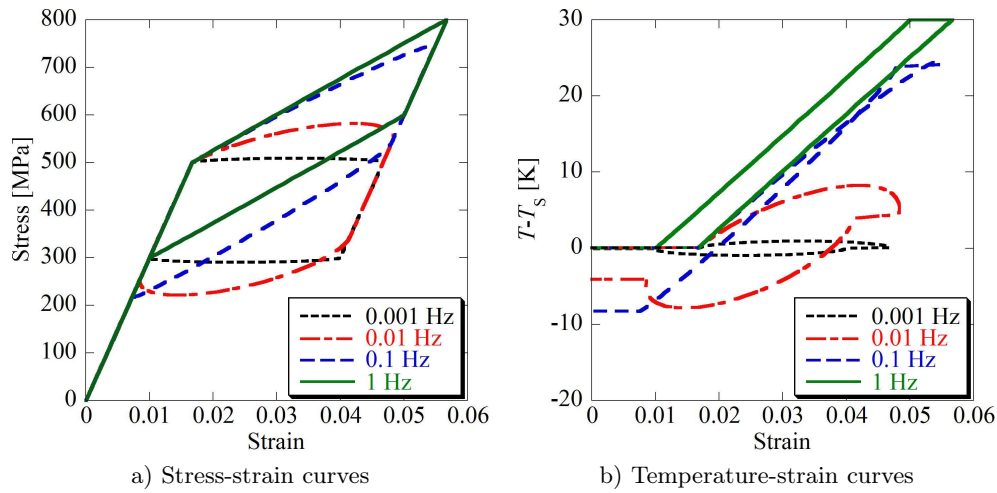


FIG. 7. Calculated stress-strain-temperature curves for various loading frequencies.

Figures 6a and 6b show stress versus volume fraction curves and temperature difference between SMA and surrounding air versus volume fraction curves, respectively, and Figs. 7a and 7b show stress versus strain curves and temperature difference versus strain curves, respectively. They are obtained by substituting the temperature calculated from Eq. (2.8) into Eq. (2.5) and Eq. (2.6) with $z_M = 0.5\{1 - \cos(2\pi ft)\}$. Here it is assumed that the elastic deformation stages are short enough not to change the temperature. Comparing these figures with Figs. 1a and 1b, it is seen that the analytical equations can also capture the stress-strain-temperature behaviour qualitatively.

3.3. Isothermal and adiabatic conditions

From Eq. (2.8) when $H \rightarrow \infty$, which corresponds to the isothermal condition

$$(3.1) \quad \Theta = 0,$$

since $e^{-Ht} \rightarrow 0$, $\Theta_2 \rightarrow 0$ and $\Theta_3 \rightarrow 0$. Accordingly, of course, the temperature does not vary.

When $H \rightarrow 0$, which corresponds to the adiabatic condition, integrating Eq. (2.7) with $H = 0$,

$$(3.2) \quad \Theta = \frac{S}{2}[1 - \cos(2\pi ft)] + F\frac{\pi f}{2}t$$

is obtained. Therefore, the temperature keeps increasing to infinity while it vibrates.

3.4. Heat generation rate

In this study it is assumed that the heat generation rate is constant during the vibration, although it is a function of $|\sin(2\pi ft)|$, since

$$(3.3) \quad \sum_{\alpha \rightarrow \beta} \Psi_{\alpha \rightarrow \beta} \frac{dz_{\alpha \rightarrow \beta}}{dt} = \Psi \pi f |\sin(2\pi ft)|.$$

When Eq. (3.3) is used instead of the assumption of constant heat generation rate, Eq. (2.7) becomes

$$(3.4) \quad \frac{d\Theta}{dt} + H\Theta = S\pi f \sin(2\pi ft) + F\pi f |\sin(2\pi ft)|.$$

This equation can be solved as

$$(3.5) \quad \Theta = \Theta_1 e^{-Ht} + \Theta_2 \sin(2\pi ft - \phi),$$

where

$$\Theta_2 = \begin{cases} \Theta_2^+ = \frac{S+F}{2} \frac{2\pi f/H}{\sqrt{(2\pi f/H)^2+1}} = \frac{S+F}{2} \sin \phi & \text{for forward transformation,} \\ \Theta_2^- = \frac{S-F}{2} \frac{2\pi f/H}{\sqrt{(2\pi f/H)^2+1}} = \frac{S-F}{2} \sin \phi & \text{for reverse transformation,} \end{cases}$$

and

$$\phi = \tan^{-1} \left(\frac{2\pi f}{H} \right).$$

Since Θ_2 for the reverse transformation takes different values from Θ_2 for the forward transformation, Θ_1 and Θ cannot be written by one formula as well, and for $0 \leq t < 1/2f$,

$$\Theta_1 = \Theta_2^+ \sin \phi = \frac{S+F}{2} \sin^2 \phi,$$

$$\Theta_2 = \Theta_2^+ = \frac{S+F}{2} \sin \phi,$$

for $1/2f \leq t < 1/f$,

$$\begin{aligned} \Theta_1 &= \Theta_2^+ \sin \phi + (\Theta_2^+ - \Theta_2^-) \sin \phi / e^{-H/(2f)} \\ &= \frac{S+F}{2} \sin^2 \phi + F \sin^2 \phi / e^{-H/(2f)}, \end{aligned}$$

$$\Theta_2 = \Theta_2^- = \frac{S-F}{2} \sin \phi,$$

and so on.

Table 4. Θ_1 , Θ_2 and ϕ for non-constant heat generation rate.

f [Hz]	Θ_1 [K]	Θ_2 [K]	ϕ [deg]	t [s]
0.1	15.1	15.3	81.0	$0 \leq t < 5$
	16.7	14.3	81.0	$5 \leq t < 10$
1	15.5	15.5	89.1	$0 \leq t < 0.5$
	16.5	14.5	89.1	$0.5 \leq t < 1$

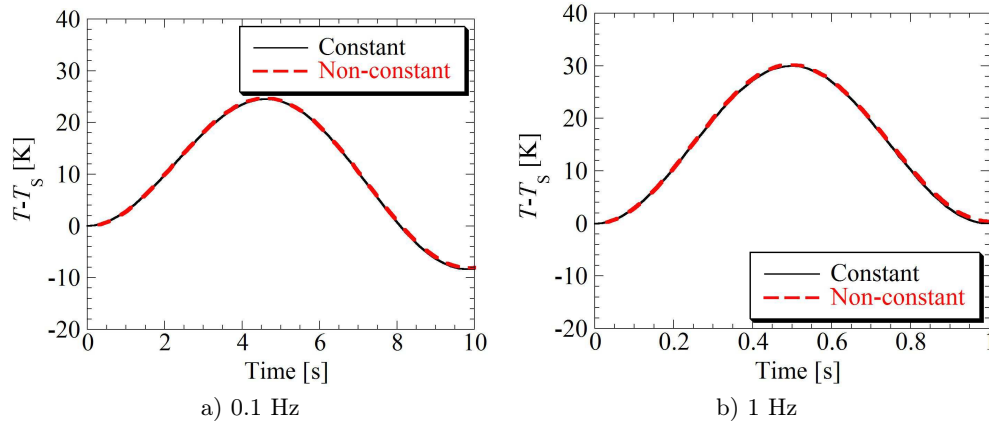


FIG. 8. Comparison in temperature variation between constant and non-constant heat generation rate.

The values of Θ_1 , Θ_2 and ϕ are listed in Table 4 for non-constant heat generation rate. In this case the meaning of Θ_1 and Θ_2 can no longer be explained directly, although the amplitude of the temperature vibration is calculated as

$$(3.6) \quad \frac{\Theta_2^+ \times 1 - \Theta_2^- \times (-1)}{2} = \frac{S}{2} \sin \phi,$$

which is the same value as the amplitude for the constant heat generation rate. The comparison of temperature vibration between Eq. (3.5) and Eq. (2.8) is shown in Figs. 8a and 8b for 0.1 Hz and 1 Hz, respectively. Their difference is not distinguished. Therefore, it is confirmed that the assumption of constant heat generation rate is reasonable.

4. Conclusions

A constitutive “one-dimensional phase transformation model” proposed by the author and his co-workers [40–43] was simplified by introducing some assumptions and the formula giving temperature variation was obtained. The factors affecting the temperature variation depending on loading frequency were analyzed from the formula. The obtained temperature variation agreed qualitatively with the measured data. The calculated stress-strain-temperature relationship also agreed qualitatively with the measured data, which indicates the proposed set of equations is reasonable.

The following findings were obtained from the formula giving temperature variation.

- (1) The temperature vibrates sinusoidally and the mean temperature approaches a certain value asymptotically.
- (2) The mean temperature decreases in a certain frequency range when the ratio of latent heat to generated heat is higher than a certain value.
- (3) The amplitude of the vibrating temperature becomes larger as the ratio of frequency to heat transfer becomes higher and converges to a half of the latent heat per heat capacity.
- (4) The mean temperature converges to a certain value calculated from the generated heat, frequency and heat transfer.
- (5) In the adiabatic condition, the temperature keeps increasing to infinity while it vibrates.

References

1. K. OTSUKA, C.M. WAYMAN (Eds.), *Shape Memory Materials*, Cambridge University Press, Cambridge, 1998.

2. K. YAMAUCHI, I. OHKATA, K. TSUCHIYA, S. MIYAZAKI (Eds.), *Shape Memory and Superelastic Alloys: Applications and Technologies*, Woodhead Publishing Limited, Oxford, Cambridge, Philadelphia, New Delhi, 2011.
3. K. OTSUKA, X. REN, *Physical metallurgy of Ti-Ni-based shape memory alloy*, Progress in Materials Science, **50**, 5, 511–678, 2005.
4. J.A. SHAW, C.B. CHURCHILL, M.A. IADICOLA, *Tips and tricks for characterizing shape memory alloy wire. Part 1. Differential scanning calorimetry and basic phenomena*, Experimental Characterization of Active Materials Series, Experimental Techniques, **32**, 5, 55–62, 2008.
5. C.B. CHURCHILL, J.A. SHAW, M.A. IADICOLA, *Tips and tricks for characterizing shape memory alloy wire. Part 2. Fundamental isothermal responses*, Experimental Characterization of Active Materials Series, Experimental Techniques, **33**, 1, 51–62, 2009.
6. C.B. CHURCHILL, J.A. SHAW, M.A. IADICOLA, *Tips and tricks for characterizing shape memory alloy wire. Part 3. Localization and propagation phenomena*, Experimental Characterization of Active Materials Series, Experimental Techniques, **33**, 5, 70–78, 2009.
7. C.B. CHURCHILL, J.A. SHAW, M.A. IADICOLA, *Tips and tricks for characterizing shape memory alloy wire. Part 4. Thermo-mechanical coupling*, Experimental Characterization of Active Materials Series, Experimental Techniques, **34**, 2, 63–80, 2010.
8. B. REEDLUNN, S. DALY, L. HECTOR, Jr., P. ZAVATTIERI, J. SHAW, *Tips and tricks for characterizing shape memory alloy wire. Part 5. Full-field strain measurement by digital image correlation*, Experimental Characterization of Active Materials Series, Experimental Techniques, **37**, 3, 62–78, 2013.
9. C. RODRIGUEZ, L.C. BROWN, *The mechanical properties of SME alloys*, [in:] Shape Memory Effects in Alloys: Proceedings of the International Symposium on Shape Memory Effects and Applications, J. Perkins (Ed.), Springer Science+Business Media, LLC, 29–58, 1975, New York.
10. J. VAN HUMBEECK, L. DELAËY, *The influence of strain-rate, amplitude and temperature on the hysteresis of a pseudoelastic Cu-Zn-Al single crystal*. Journal de Physique Colloques, **42**, C5, C5-1007-C5-1011, 1981.
11. P.H. LEO, T.W. SIELD, O.P. BRUNO, Transient heat transfer effects on the pseudoelastic behavior of shape-memory wires, Acta Metallurgica, **41**, 8, 2477–2485, 1993.
12. P.H. LIN, H. TOBUSHI, K. TANAKA, T. HATTORI, A. IKAI, *Influence of strain rate on deformation properties of TiNi shape memory alloy*, JSME International Journal, Series A, **39**, 1, 117–123, 1996.
13. Y. LIU, J. VAN HUMBEECK, *On the damping behaviour of NiTi shape memory alloy*, Journal de Physique IV, **7**, C5, C5-519-C5-524, 1997.
14. F. GANDHI, D. WOLONS, *Characterization of the pseudoelastic damping behavior of shape memory alloy wires using complex modulus*, Smart Materials and Structures, **8**, 1, 49–56, 1999.
15. H. NAITO, Y. MATSUZAKI, T. IKEDA, T. SASAKI, *Experimental and analytical studies on stress-strain-temperature relationship of NiTi shape memory alloy subjected to cycling loadings*, Transactions of the JSME (A), **69**, 679, 515–522, 2003 (in Japanese).
16. Y.J. HE, Q.P. SUN, *Frequency-dependent temperature evolution in NiTi shape memory alloy under cyclic loading*, Smart Materials and Structures, **19**, 11, 115014 (9 pp), 2010.

17. H. YIN, Y. HE, Q. SUN, *Effect of deformation frequency on temperature and stress oscillations in cyclic phase transition of NiTi shape memory alloy*, Journal of the Mechanics and Physics of Solids, **67**, 100–128, 2014.
18. L.G. MACHADO, D.C. LAGODAS, *Thermomechanical constitutive modeling of SMAs*, Shape Memory Alloys – Modeling and Engineering Applications, D.C. Lagoudas (Ed.), Springer Science + Business Media, LLC, 121–187, 2008, New York.
19. S. BARBARINO, E.I. SAAVEDRA FLORES, R.M. AJAJ, I. DAYYANI, M.I. FRISWELL, *A review on shape memory alloys with applications to morphing aircraft*, Smart Materials and Structures, **23**, 6, 063001 (19 pp), 2014.
20. F. FALK, *One-dimensional model of shape memory alloys*, Archives of Mechanics, **35**, 1, 63–84, 1983.
21. I. Müller, *On the size of the hysteresis in pseudoelasticity*, Continuum Mechanics and Thermodynamics, **1**, 2, 125–142, 1989.
22. S. SEELECKE, *Equilibrium thermodynamics of pseudoelasticity and quasiplasticity*, Continuum Mechanics and Thermodynamics, **8**, 5, 309–322, 1996.
23. A. BERTRAM, *Thermo-mechanical constitutive equations for the description of shape memory effects in alloys*, Nuclear Engineering and Design, **74**, 2, 173–182, 1982.
24. K. TANAKA, *A thermomechanical sketch of shape memory effect: one-dimensional tensile behavior*, Res Mechanica, **18**, 3, 251–263, 1986.
25. C. LIANG, C.A. ROGERS, *One-dimensional thermomechanical constitutive relations for shape memory materials*, Journal of Intelligent Material Systems and Structures, **1**, 2, 207–234, 1990.
26. L.C. BRINSON, *One-dimensional constitutive behavior of shape memory alloys: thermomechanical derivation with non-constant material functions and redefined martensite internal variable*, Journal of Intelligent Material Systems and Structures, **4**, 2, 229–242, 1993.
27. Q.P. SUN, K.C. HWANG, *Micromechanics modelling for the constitutive behavior of polycrystalline shape memory alloys – I. derivation of general relations*, Journal of the Mechanical Physics of Solids, **41**, 1, 1–17, 1993.
28. J.G. BOYD, D.C. LAGODAS, *A thermodynamical constitutive model for shape memory materials. part I. the monolithic shape memory alloy*, International Journal of Plasticity, **12**, 6, 805–842, 1996.
29. B. RANIECKI, C.H. LEXCELLENT, K. TANAKA, *Thermodynamic models of pseudoelastic behavior of shape memory alloys*, Archives of Mechanics, **44**, 3, 261–284, 1992.
30. Y. IVSHIN, T.J. PENCE, *A thermomechanical model for a one variant shape memory material*, Journal of Intelligent Material Systems and Structures, **5**, 4, 455–473, 1994.
31. S. LECLERCQ, C. LEXCELLENT, *A general macroscopic description of the thermomechanical behavior of shape memory alloys*, Journal of the Mechanics and Physics of Solids, **44**, 6, 953–980, 1996.
32. T. KAMITA, Y. MATSUZAKI, *One-dimensional pseudoelastic theory of shape memory alloys*, Smart Materials and Structures, **7**, 4, 489–495, 1998.
33. Y. MATSUZAKI, H. NAITO, T. IKEDA, K. FUNAMI, *Thermo-mechanical behavior associated with pseudoelastic transformation of shape memory alloys*, Smart Materials and Structures, **10**, 5, 884–892, 2001.

34. F. AURICCHIO, E. SACCO, *Thermo-mechanical modelling of a superelastic shape-memory wire under cyclic stretching-bending loadings*, International Journal of Solids and Structures, **38**, 34-35, 6123–6145, 2001.
35. E. PATOOR, A. EBERHARDT, M. BERVEILLER, *Micromechanical modelling of the superelastic behavior*, Journal de Physique IV, **5**, C2, C-2-501-C2-506, 1995.
36. K. GALL, H. SEHITOGLU, *The role of texture in tension-compression asymmetry in polycrystalline NiTi*, International Journal of Plasticity, **15**, 1, 69–92, 1999.
37. F.A. NAE, Y. MATSUZAKI, T. IKEDA, *Micromechanical modeling of polycrystalline shape-memory alloys including thermo-mechanical coupling*, Smart Materials and Structures, **12**, 1, 6–17, 2003.
38. E.J. GRAESSER, F.A. COZZARELLI, *Shape-memory alloys as new materials for aseismic isolation*, Journal of Engineering Mechanics, **117**, 11, 2590–2608, 1991.
39. J. ORTÍN, *Preisach modeling of hysteresis for a pseudoelastic Cu-Zn-Al single crystal*, Journal of Applied Physics, **71**, 3, 1454–1461, 1992.
40. T. IKEDA, F.A. NAE, H. NAITO, Y. MATSUZAKI, *Constitutive model of shape memory alloys for unidirectional loading considering inner hysteresis loops*, Smart Materials and Structures, **13**, 4, 916–925, 2004.
41. T. IKEDA, *Modeling of ferroelastic behavior of shape memory alloys*, [in:] Proceedings of SPIE, **5757**, 344–352, 2005.
42. T. IKEDA, *Constitutive model of shape memory alloys for asymmetric quasiplastic behavior*, Journal of Intelligent Material Systems and Structures, **19**, 5, 533–540, 2008.
43. T. IKEDA, *Application of one-dimensional phase transformation model to tensile-torsional pseudoelastic behavior of shape memory alloy tubes*, [in:] Proceedings of SPIE, **6166**, 6166Z (8 pp), 2006.
44. T. IKEDA, H. HATTORI, Y. MATSUZAKI, *Numerical analysis of damping enhancement of a beam with shape memory alloy foils bonded*, [in:] Proceedings of ICAS 2004, ICAS 2004-5.2.1 (8 pp), 2004.

Received October 5, 2014; revised version May 15, 2015.
